

## Polarization of $\Sigma^+$ and $\bar{\Sigma}^-$ Hyperons Produced by 800-GeV/c Protons

A. Morelos,<sup>1,\*</sup> I. F. Albuquerque,<sup>12</sup> N. F. Bondar,<sup>2</sup> R. A. Carrigan, Jr.,<sup>1</sup> D. Chen,<sup>8,†</sup> P. S. Cooper,<sup>1</sup> Dai Lisheng,<sup>3</sup> A. S. Denisov,<sup>2</sup> A. V. Dobrovolsky,<sup>2</sup> T. Dubbs,<sup>6</sup> A. M. F. Endler,<sup>10</sup> C. O. Escobar,<sup>12</sup> M. Foucher,<sup>13,‡</sup> V. L. Golovtsov,<sup>2</sup> H. Gottschalk,<sup>12</sup> P. Gouffon,<sup>12</sup> V. T. Grachev,<sup>2</sup> A. V. Khanzadeev,<sup>2</sup> M. A. Kubantsev,<sup>7</sup> N. P. Kuropatkin,<sup>2</sup> J. Lach,<sup>1</sup> Lang Pengfei,<sup>3</sup> Li Chengze,<sup>3</sup> Li Yunshan,<sup>3</sup> M. Luksys,<sup>9,§</sup> J. R. P. Mahon,<sup>12</sup> E. McCliment,<sup>6</sup> C. Newsom,<sup>6</sup> M. C. Pomot Maia,<sup>11,||</sup> V. M. Samsonov,<sup>2</sup> V. A. Schegelsky,<sup>2</sup> Shi Huanzhang,<sup>3</sup> V. J. Smith,<sup>4</sup> Tang Fukun,<sup>3</sup> N. K. Terentyev,<sup>2</sup> S. Timm,<sup>5</sup> I. I. Tkatch,<sup>2</sup> L. N. Uvarov,<sup>2</sup> A. A. Vorobyov,<sup>2</sup> Yan Jie,<sup>3</sup> Zhao Wenheng,<sup>3</sup> Zheng Shuchen,<sup>3</sup> and Zhong Yuanyuan<sup>3</sup>

(E761 Collaboration)

<sup>1</sup>Fermi National Accelerator Laboratory, Batavia, Illinois 60510

<sup>2</sup>Petersburg Nuclear Physics Institute, Gatchina, Russia

<sup>3</sup>Institute of High Energy Physics, Beijing, People's Republic of China

<sup>4</sup>H. H. Wills Physics Laboratory, University of Bristol, Bristol, United Kingdom

<sup>5</sup>Carnegie Mellon University, Pittsburgh, Pennsylvania 15213

<sup>6</sup>University of Iowa, Iowa City, Iowa 52242

<sup>7</sup>Institute of Theoretical and Experimental Physics, Moscow, Russia

<sup>8</sup>State University of New York at Albany, Albany, New York 12222

<sup>9</sup>Universidade Federal da Paraiba, Paraiba, Brazil

<sup>10</sup>Centro Brasileiro de Pesquisas Fisicas, Rio de Janeiro, Brazil

<sup>11</sup>Conselho Nacional de Pesquisas (CNPq), Rio de Janeiro, Brazil

<sup>12</sup>Universidade de São Paulo, São Paulo, Brazil

<sup>13</sup>J. W. Gibbs Laboratory, Yale University, New Haven, Connecticut 06511

(Received 25 March 1993)

We have measured the polarization of 375-GeV/c  $\Sigma^+$  and  $\bar{\Sigma}^-$  hyperons produced by 800-GeV/c protons incident on a Cu target. We find that the  $\Sigma^+$  polarization rises with increasing  $p_t$  to a maximum of 16% at  $p_t = 1.0$  GeV/c and then decreases to 10% at  $p_t = 1.8$  GeV/c. We compare this  $\Sigma^+$  polarization with data at lower energies. The  $\bar{\Sigma}^-$  polarization has been measured for the first time. It has the same sign as the  $\Sigma^+$  but smaller magnitude in a similar kinematical region.

PACS numbers: 13.85.Ni, 13.88.+e

The inclusive production of hyperons by high energy protons [1,2] has provided us with copious sources of hyperons with controlled polarization. These reactions have a rich and complicated structure and the mechanism responsible for the polarization is not well understood.

Studies [3–6] of the  $\Lambda^0$  and  $\bar{\Lambda}^0$  polarization using 300- and 400-GeV/c protons incident on a Be target at Fermilab provided a benchmark for the comparison of other reactions. The  $\Lambda^0$  polarization was found to be zero [7,8] in the forward direction (as required by rotational symmetry for production from an unpolarized beam and target) and decreased linearly to  $\approx -25\%$  at a transverse momentum ( $p_t$ ) of  $\approx 1.0$  GeV/c. We use the conventional sign definition [9] for the inclusive hyperon polarization: A positive polarization is in the same direction as the cross product of the incident beam direction with the produced hyperon direction. At larger  $p_t$  the polarization was approximately constant. Although reliable theoretical predictions of their polarizations cannot be made at these  $p_t$  values, QCD predictions [10] expect it to vanish at large  $p_t$ . These experiments also found that the polarization [2] was independent of the initial proton energy and had little dependence on the target material.

The  $\bar{\Lambda}^0$  polarization was found to be consistent with zero in the same kinematical regions that have significant

$\Lambda^0$  polarization. These polarizations have generally been attributed to peripheral mechanisms [11–17] in which some of the proton valence quarks assimilate a strange quark from the sea to form a polarized hyperon. The  $\bar{\Lambda}^0$  does not contain any of the valence quarks of the proton projectile and that might explain the absence of polarization in this case.

The conjecture that the more quarks incorporated from the sea reduces the produced hyperon polarization seemed to be confirmed by measurements of the polarization [18–27] of  $\Sigma^\pm$ ,  $\Xi^-$ , and  $\Omega^-$  hyperons but apparently not [28] for  $\Xi^0$ . However, recent measurements of  $\Xi^-$  and  $\bar{\Xi}^+$  polarizations [29,30] using an 800-GeV/c proton beam incident on a Be target indicate that both are polarized with the same sign and similar magnitudes. This differs dramatically from the behavior of the  $\Lambda^0/\bar{\Lambda}^0$  system and confounds the interpretation as being attributable to peripheral mechanisms. In this experiment we investigated the  $\Sigma^+/\bar{\Sigma}^-$  system in the hope of shedding more light on these polarization mechanisms. These measurements [31] were performed as part of a Fermilab experiment (E761) which was designed to measure the asymmetry parameter [32] in the decay  $\Sigma^+ \rightarrow p\gamma$ .

Figure 1 shows the relevant parts of the E761 apparatus [31–33] located in the Proton Center beam line

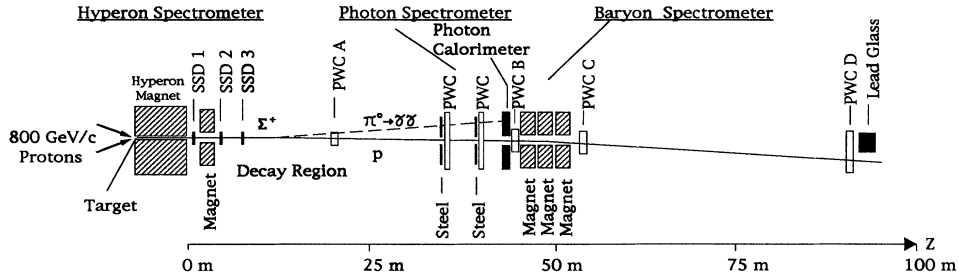


FIG. 1. Plan view of the apparatus showing the incident proton beam, hyperon, baryon, and photon spectrometers.

at Fermilab and used in these measurements. The configuration and experimental resolutions are the same as in the asymmetry parameter measurement [32] and all of these data were collected during that run. This study used the  $\Sigma^+ \rightarrow p\pi^0$  ( $\bar{\Sigma}^- \rightarrow \bar{p}\pi^0$ ) decay mode for analysis of the  $\Sigma^+$  ( $\bar{\Sigma}^-$ ) polarization.

The apparatus, shown in Fig. 1, included a hyperon spectrometer [one dipole magnet and three clusters of silicon strip detectors (SSD)] and a baryon spectrometer [three dipole magnets and four clusters of multiwire proportional chamber (PWC)]. A photon spectrometer converted photons in two 2.54-cm-thick steel plates ( $\approx 1.5$  radiation lengths each) and measured the photon energy in a lead-glass-bismuth-germanate (BGO) calorimeter. There was a  $76 \times 76\text{-mm}^2$  hole in the photon spectrometer (including steel plates and calorimeter) to allow the undecayed beam and the baryon through. This angular region was covered by a downstream lead-glass array.

Protons of 800 GeV/c were steered and focused onto the hyperon production target. The charged hyperon beam originated from a 1-interaction-length Cu target in the upstream end of a 7.3-m-long hyperon magnet which imparted a transverse momentum of about  $-7.5$  GeV/c to the 375-GeV/c hyperon beam. Dipole magnets upstream of the target (not shown in Fig. 1) could vary the targeting angle over the range  $\approx \pm 5$  mrad in either the horizontal or vertical plane. This allowed for hyperons to be produced, in a controlled manner, with their respective

polarization directions either parallel or perpendicular to the vertical magnetic field of the hyperon magnet (Fig. 1). These two conditions correspond to no hyperon spin precession or maximal spin precession, respectively, in the hyperon magnet. The currents in all of the magnets shown in Fig. 1 could be reversed, thus allowing selection of a positive or negative beam.

The trigger consisted of scintillation counters in each of the three spectrometers. A hyperon candidate was defined as an event with a particle in the incident beam and a baryon candidate detected by a scintillator signal in a region where protons (antiprotons) from  $\Sigma^+$  ( $\bar{\Sigma}^-$ ) decay were expected. The trigger also required a combination of scintillators in the photon spectrometer indicating the conversion of a photon in the steel plates, and the detection of  $> 5$  GeV in the photon calorimeter. The photon spectrometer information was used in the trigger but was not used in further analysis for the physics presented here. The geometrical acceptance of the apparatus was  $\approx 85\%$  for  $\Sigma^+ \rightarrow p\pi^0$  and  $\bar{\Sigma}^- \rightarrow \bar{p}\pi^0$  which decayed in a decay region (Fig. 1) defined from SSD 3 to PWC A.

The mode [34] responsible for 52% of the  $\Sigma^+$  decays,  $\Sigma^+ \rightarrow p\pi^0$ , was identified by measuring the vector momentum of the  $\Sigma^+$  in the hyperon spectrometer and the proton in the baryon spectrometer. This decay mode has a large asymmetry parameter [34],  $\alpha = -0.980 \pm 0.016$ , making it a sensitive analyzer of  $\Sigma^+$  polarization. In the negative beam the identification of the  $\bar{\Sigma}^- \rightarrow \bar{p}\pi^0$  was ac-

TABLE I. Experimental data.

Mode	Particle	$\langle \text{Angle} \rangle$ (mrad)	Events	$\langle p_t \rangle$ (GeV/c)	Polarization
H	$\bar{\Sigma}^-$	$\pm 2.8$	28 957	$1.07 \pm 0.09$	$0.068 \pm 0.011$
H	$\bar{\Sigma}^-$	$\pm 1.8$	23 630	$0.68 \pm 0.09$	$0.088 \pm 0.011$
H	$\bar{\Sigma}^-$	$\pm 0.9$	1 554	$0.33 \pm 0.10$	$0.048 \pm 0.045$
V	$\bar{\Sigma}^-$	$\pm 2.9$	11 806	$1.07 \pm 0.07$	$0.072 \pm 0.017$
H	$\Sigma^+$	$\pm 4.8$	23 744	$1.80 \pm 0.07$	$0.104 \pm 0.011$
H	$\Sigma^+$	$\pm 4.3$	23 173	$1.64 \pm 0.07$	$0.112 \pm 0.012$
H	$\Sigma^+$	$\pm 3.7$	43 225	$1.40 \pm 0.07$	$0.112 \pm 0.010$
H	$\Sigma^+$	$\pm 3.7$	12 573 218	$1.40 \pm 0.07$	$0.124 \pm 0.001$
H	$\Sigma^+$	$\pm 3.3$	20 351	$1.24 \pm 0.08$	$0.131 \pm 0.012$
H	$\Sigma^+$	$\pm 0.9$	14 134	$0.35 \pm 0.10$	$0.106 \pm 0.015$
V	$\Sigma^+$	$\pm 2.9$	249 863	$1.08 \pm 0.07$	$0.163 \pm 0.004$

completed in a similar manner. We assume [35] the masses of the hyperons are the same as the antihyperons and their asymmetry parameters have identical magnitudes but opposite signs.

Approximately equal amounts of data were collected at pairs of targeting angles as shown in Table I. The targeting angles were of equal magnitude but opposite signs, thus allowing the polarization to be periodically reversed to separate the asymmetry (the asymmetry is the product of the asymmetry parameter  $\alpha$  and the polarization) from instrumental biases. In Table I we include  $\Sigma^+$  and  $\bar{\Sigma}^-$  data from both horizontal (H) and vertical (V) targeting. The measurement of the asymmetry parameter [32] in the decay  $\Sigma^+ \rightarrow p\gamma$  included a large data sample of  $\Sigma^+ \rightarrow p\pi^0$  decays which we also used for a measurement of polarization at  $\pm 3.7$  mrad. Events were reconstructed assuming the incident particle was a  $\Sigma^+$  and the trajectory in the baryon spectrometer was that of a proton. The decay position,  $z_v$ , of the  $\Sigma^+$  as well as  $\Theta$ , the proton laboratory decay angle relative to the  $\Sigma^+$  direction, were determined. Goodness of fit criteria on the proton and

hyperon tracks, a restriction that  $\Theta > 0.1$  mrad, and a requirement that the reconstructed vertex be in the fiducial region were imposed on the event samples. Figure 2(a) shows a mass squared distribution ( $M_{X^0}^2$ ) of the missing neutral particle ( $X^0$ ) for the hypothesis  $\Sigma^+ \rightarrow pX^0$  after the above  $\Theta$  and  $z_v$  selections. The center and width of the  $\pi^0$  signal are in agreement with the expected position and resolution. Figure 2(b) shows the equivalent distribution of the negative beam. The small background from the kaon decays at high  $M_{X^0}^2$  and the even smaller background from radiative decays at low  $M_{X^0}^2$  do not significantly affect our polarization measurements. However, the data of Fig. 2 were subjected to additional selection criteria. These included rejection of events where the proton trajectory was near the edges of the hole in the photon spectrometer and rejection of events whose reconstructed neutral mass assuming a decay  $K^+ \rightarrow \pi^+\pi^0$  ( $K^- \rightarrow \pi^-\pi^0$ ) was near the  $\pi^0$  mass. A final requirement was that the reconstructed missing neutral particle ( $X^0$ ) be in the range  $0.010 < M_{X^0}^2 < 0.026$  ( $\text{GeV}/c^2$ )<sup>2</sup>. The final event sample is described in Table I.

In Table I the quoted uncertainty in the polarization is statistical. We studied the sensitivity of our result to variations of our selection criteria in  $\Theta$ ,  $M_{X^0}^2$ , and  $z_v$  position and angle in the beam phase space using our higher statistics samples. These systematic uncertainties, which

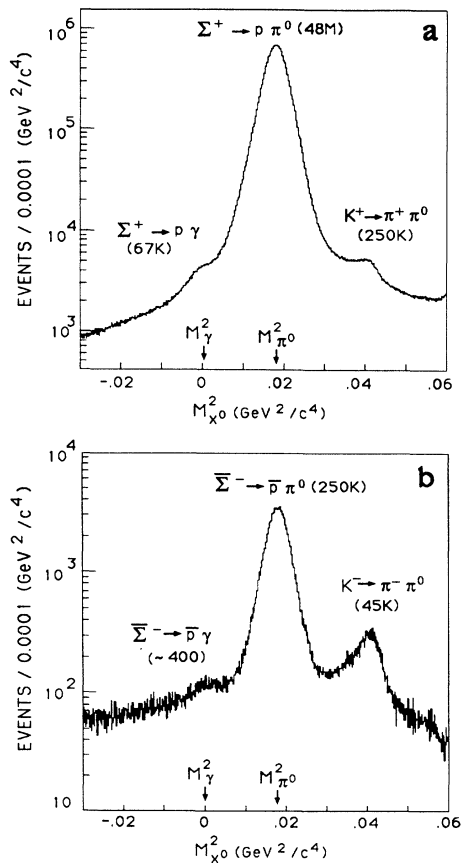


FIG. 2. (a) Event distributions of the mass squared of the missing neutral particle ( $X^0$ ) for the hypothesis  $\Sigma^+ \rightarrow pX^0$  for all positive beam candidates. (b) Event distributions of the mass squared of the missing neutral particle ( $X^0$ ) for the hypothesis  $\bar{\Sigma}^- \rightarrow \bar{p}X^0$  for all negative beam candidates.

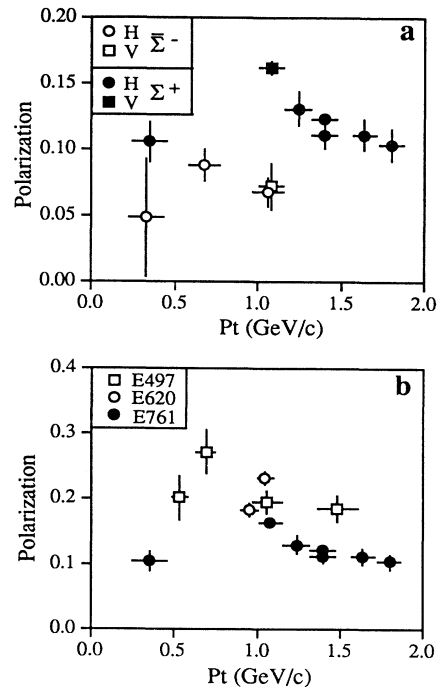


FIG. 3. (a) Comparison of polarizations for  $\Sigma^+$  and  $\bar{\Sigma}^-$  as a function of  $p_t$  from this experiment. (b) Polarization of  $\Sigma^+$  as a function of  $p_t$  and comparison with previous measurements at 400-GeV incident proton energy. Note that the E620 data are from production on a Be target. The others use a Cu target. All of these data are in the range  $0.47 < x_F < 0.53$ .

we estimated as 0.0032, were combined in quadrature with the statistical uncertainty and are included in Fig. 3. We treat the uncertainty [34] in the value of  $\alpha$  ( $\pm 1.6\%$ ) as a scale factor in these measurements which is not included in our stated systematic uncertainty.

From Table I, it is clear that both the  $\Sigma^+$  and  $\bar{\Sigma}^-$  are produced polarized. At similar values of  $p_t$  the polarizations have the same sign but different magnitudes. These polarizations are plotted in Fig. 3(a) as functions of  $p_t$ . The horizontal error bar is the rms width of the  $p_t$  distribution at that production angle.

One can see the  $\Sigma^+$  polarization increasing with  $p_t$ , reaching a maximum at  $p_t \approx 1$  GeV/c, and then decreasing. This is the first clear experimental indication that high energy hyperon polarization decreases at large  $p_t$ . The  $\bar{\Sigma}^-$  polarization data are consistent with a similar behavior.

How does the  $\Sigma^+$  polarization depend on the incident proton energy? Comparisons with other Fermilab  $\Sigma^+$  polarization measurements [18,19] are shown in Fig. 3(b). In order to minimize the effects of the  $x_F$  polarization dependence, we choose only data within the range  $0.47 < x_F < 0.53$  ( $x_F$  being the ratio of the hyperon momentum divided by the incident proton momentum). The magnitudes of the 800-GeV polarizations are less than those at 400 GeV indicating a clear energy dependence of the  $\Sigma^+$  polarization in that kinematical region. This can be seen from data which use only Cu targets (all but the E620 data [19]). The two plotted E620 data points would indicate a large  $x_F$  dependence since they differ in  $x_F$  by only 0.05. Recent results [29] on the  $\Xi^-$  also indicate an energy dependence of the polarization. In contrast to the  $\Sigma^+$ , the polarization magnitude of the  $\Xi^-$  increases as the incident proton energy increases from 400 to 800 GeV.

This experiment demonstrated that  $\bar{\Sigma}^-$  hyperons are produced in high energy collisions with polarization of the same sign though of smaller magnitude than that of  $\Sigma^+$ . This observation is similar to the recent Fermilab results [30] which showed that both  $\Xi^-$  and  $\bar{\Xi}^+$  are polarized with about the same magnitude. This would indicate that the polarization of antihyperons is a common phenomenon, and we should now turn our attention to why the  $\bar{\Lambda}^0$  are not produced polarized.

Our data indicate that the  $\Sigma^+$  polarization at our energy starts to decrease at large  $p_t$ . We have also shown that the  $\Sigma^+$  polarization magnitude decreases with incident energy in contrast to the  $\Xi^-$ , which increases [29] with incident energy.

Clearly the  $\Lambda^0/\bar{\Lambda}^0$ ,  $\Xi^-/\bar{\Xi}^+$ , and  $\Sigma^+/\bar{\Sigma}^-$  systems exhibit a rich and challenging set of polarization phenomena that cry out for insightful ideas.

We wish to thank the staffs of Fermilab and the Petersburg Nuclear Physics Institute for their assistance. This work is supported in part by the U.S. Department of Energy under Contracts No. DE-AC02-76CH03000, No. DE-AC02-76ER03075, No. DE-FG02-91ER40664, No.

DE-FG02-91ER40682, and No. DE-FG02-91ER40631, the Russian Academy of Sciences, and the U.K. Science and Engineering Research Council. A.M. was partially supported by CONACyT, Mexico. I.F.A. was supported by FAPESP, Brazil. P.G. and J.R.P.M. were partially supported by FAPESP and CNPq, Brazil.

\*Now at the Superconducting Super Collider Laboratory, Dallas, TX 75237.

†Now at Fermilab, Batavia, IL 60510.

‡Present address: Department of Physics, University of Maryland, College Park, MD 20742.

§Present address: Universidade de São Paulo, São Paulo, Brazil.

¶Present address: Department of Physics, Stanford University, Stanford, CA 94309.

- [1] J. Lach and L. Pondrom, *Annu. Rev. Nucl. Part. Sci.* **29**, 203 (1979).
- [2] L. Pondrom, *Phys. Rep.* **122**, 57 (1985).
- [3] G. Bunce *et al.*, *Phys. Rev. Lett.* **36**, 1113 (1976).
- [4] K. Heller *et al.*, *Phys. Rev. Lett.* **41**, 607 (1978).
- [5] P. Skubic *et al.*, *Phys. Rev. D* **18**, 3115 (1978).
- [6] B. Lundberg *et al.*, *Phys. Rev. D* **40**, 3557 (1989).
- [7] P. Yamin *et al.*, *Phys. Rev. D* **23**, 31 (1981).
- [8] K. Heller *et al.*, *Phys. Rev. Lett.* **51**, 2025 (1983).
- [9] Special issue on the Basel Convention [*Helv. Phys. Acta*, Suppl. VI (1961)].
- [10] G. L. Kane *et al.*, *Phys. Rev. Lett.* **41**, 1689 (1978).
- [11] T. A. DeGrand and H. I. Miettinen, *Phys. Rev. D* **24**, 2419 (1981).
- [12] B. Andersson *et al.*, *Phys. Lett.* **85B**, 417 (1979).
- [13] J. Szwed, *Phys. Lett.* **105B**, 403 (1981).
- [14] P. Cea *et al.*, *Phys. Lett. B* **209**, 333 (1988).
- [15] J. Soffer and N. A. Tornqvist, *Phys. Rev. Lett.* **68**, 907 (1992).
- [16] W. G. D. Dharmaratna and G. R. Goldstein, *Phys. Rev. D* **41**, 1731 (1990).
- [17] R. Barni *et al.*, *Phys. Lett. B* **296**, 251 (1992).
- [18] C. Ankenbrandt *et al.*, *Phys. Rev. Lett.* **51**, 863 (1983).
- [19] C. Wilkinson *et al.*, *Phys. Rev. Lett.* **58**, 855 (1987).
- [20] Y. W. Wah *et al.*, *Phys. Rev. Lett.* **55**, 2551 (1985).
- [21] L. Deck *et al.*, *Phys. Rev. D* **28**, 1 (1983).
- [22] G. Zapalac *et al.*, *Phys. Rev. Lett.* **57**, 1526 (1986).
- [23] R. Rameika *et al.*, *Phys. Rev. D* **33**, 3172 (1986).
- [24] L. H. Trost *et al.*, *Phys. Rev. D* **40**, 1703 (1989).
- [25] H. T. Diehl *et al.*, *Phys. Rev. Lett.* **67**, 804 (1991).
- [26] K. B. Luk *et al.*, *Phys. Rev. D* **38**, 19 (1988).
- [27] K. B. Luk *et al.*, *Phys. Rev. Lett.* **70**, 900 (1993).
- [28] A. Beretvas *et al.*, *Phys. Rev. D* **34**, 53 (1986).
- [29] J. Duryea *et al.*, *Phys. Rev. Lett.* **67**, 1193 (1991).
- [30] P. M. Ho *et al.*, *Phys. Rev. Lett.* **65**, 1713 (1990).
- [31] A. Morelos, Ph.D. thesis, Centro de Investigacion y de Estudios Avanzados del IPN, Mexico, 1992 (unpublished).
- [32] M. Foucher *et al.*, *Phys. Rev. Lett.* **68**, 3004 (1992).
- [33] D. Chen *et al.*, *Phys. Rev. Lett.* **69**, 3286 (1992).
- [34] Particle Data Group, K. Hikasa *et al.*, *Phys. Rev. D* **45**, S1 (1992).
- [35] T. D. Lee *et al.*, *Phys. Rev.* **106**, 340 (1957).